

# Dynamical quantum phase transitions in the dissipative Lipkin-Meshkov-Glick model with proposed realization in optical cavity QED

S. Morrison<sup>1,2</sup> and A. S. Parkins<sup>3</sup>

<sup>1</sup>*Institute for Theoretical Physics, University of Innsbruck, Innsbruck A-6020, Austria*

<sup>2</sup>*Institute for Quantum Optics and Quantum Information of the Austrian Academy of Sciences, A-6020 Innsbruck, Austria*

<sup>3</sup>*Department of Physics, University of Auckland, Private Bag 92019, Auckland, New Zealand*

(Dated: February 4, 2008)

We present an optical cavity QED configuration that is described by a dissipative version of the Lipkin-Meshkov-Glick model of an infinitely coordinated spin system. This open quantum system exhibits both first- and second-order non-equilibrium quantum phase transitions as a single, effective field parameter is varied. Light emitted from the cavity offers measurable signatures of the critical behavior, including that of the spin-spin entanglement.

PACS numbers: 42.50.Fx, 42.50.Pq, 03.65.Ud, 73.43.Nq

Remarkable advances with trapped, ultra-cold atomic gases have opened up exciting new avenues of research into strongly interacting many-body quantum systems [1]. Exquisite control of both motional and electronic degrees of freedom of cold atoms can enable one to “tailor” atom-atom interactions and thereby implement a variety of systems that exhibit, in particular, quantum critical phenomena, i.e., transitions between distinct quantum phases, driven by quantum fluctuations, in response to variations of an effective field or interaction strength around some critical value.

Recently, important insights into such transitions have been obtained from theoretical studies of the quantum entanglement properties of critical spin systems (see, e.g., [2, 3, 4, 5, 6, 7, 8, 9, 10]). Bipartite entanglement measures characterizing entanglement between a pair of spins (e.g., the concurrence) or between two blocks of spins (e.g., the entanglement entropy) can display marked critical behavior and scaling at quantum critical points. In this context, a simple but very useful example is the Lipkin-Meshkov-Glick (LMG) model [11], which is described by the Hamiltonian

$$H_{\text{LMG}} = -2hJ_z - (2\lambda/N)(J_x^2 + \gamma J_y^2), \quad (1)$$

where  $\{J_x, J_y, J_z\}$  are collective angular momentum operators for  $N$  spin-1/2 particles,  $h$  and  $\lambda$  are effective magnetic field and spin-spin interaction strengths, respectively, and  $\gamma \in [-1, 1]$  is an anisotropy parameter. This system, in which each spin interacts identically with every other spin, exhibits critical behavior at zero temperature; in particular, either first- or second-order equilibrium quantum phase transitions may occur, depending on the choice of  $\lambda$  and  $\gamma$ , as the ratio  $h/\lambda$  is varied across a critical value [6]. Notably, the second-order transition involves a change from a unique ground state (normal phase) to a pair of macroscopically displaced degenerate ground states (broken phase). Entanglement in the system displays the above-mentioned critical behavior, reaching, in particular, a pronounced maximum at the critical point [5, 6, 7].

Given these interesting and topical features of the LMG model, it follows that the physical realization of a system described by such a model would provide a valuable test bed for studies of quantum critical phenomena and entanglement. Here we propose an open-system (i.e., dissipative) version of the LMG model based on the collective interaction of an ensemble of atoms with laser fields and field modes of a high-finesse optical resonator. In the spirit of a recent proposal for realizing the Dicke model [12], our scheme employs Raman transitions between a pair of atomic ground states and the relevant energy scales (e.g.,  $h$ ,  $\lambda$ ) are set by light shifts of the atomic levels and Raman transition rates and detunings.

The open nature of this system, a consequence of the external driving fields and cavity mode losses, introduces a number of important differences from, and, arguably, advantages over, the closed, Hamiltonian LMG system: (i) thermal equilibrium phase transitions are replaced by dynamical, non-equilibrium phase transitions, (ii) the cavity output fields offer quantitative measures of properties of the collective-spin system, including entanglement, in the critical regime, and (iii) it is possible to observe both first- and second-order quantum phase transitions as a *single effective field parameter,  $h$ , is varied*.

We consider  $N$  atoms coupled via electric dipole transitions to three laser fields and to a pair of independent (e.g., orthogonally-polarized) optical cavity modes. The atomic level and excitation scheme is shown in Fig. 1, together with a possible ring-cavity setup. At the location of the atoms, the cavity and laser fields are copropagating traveling waves, with sufficiently broad beam waists so as to ensure homogeneous atom-field couplings. These fields combine to drive Raman transitions between two stable electronic ground states of the atoms,  $|0\rangle$  and  $|1\rangle$  (energies  $\omega_0 = 0$  and  $\omega_1$ , respectively, with  $\hbar = 1$ ) via the excited atomic states  $|r\rangle$  and  $|s\rangle$  (energies  $\omega_r$  and  $\omega_s$ ). The laser fields have optical frequencies  $\omega_{r0}$ ,  $\omega_{s0}$ , and  $\omega_{r1}$ , and couple to the atomic transitions with Rabi frequencies  $\Omega_{r0}$ ,  $\Omega_{s0}$ , and  $\Omega_{r1}$ . Cavity field  $a$ , at frequency  $\omega_a$ , couples to the transitions  $|0\rangle \leftrightarrow |r\rangle$  and

$|1\rangle \leftrightarrow |s\rangle$  with strengths  $g_{r0}$  and  $g_{s1}$ , respectively, while cavity field  $b$ , at frequency  $\omega_b$ , couples to the transitions  $|0\rangle \leftrightarrow |s\rangle$  and  $|1\rangle \leftrightarrow |r\rangle$  with strengths  $g_{s0}$  and  $g_{r1}$ , respectively. As drawn in Fig. 1, the level scheme would apply, e.g., to  ${}^6\text{Li}$ , with the ground magnetic substates  $|F = 1/2, m = \pm 1/2\rangle$  as  $|0\rangle$  and  $|1\rangle$  and a magnetic field perpendicular to the cavity axis to provide a splitting  $\omega_1$  between these states. Modes  $a$  and  $b$  would be orthogonal, linearly-polarized cavity modes, with mode  $a$  polarized along the direction of the magnetic field.

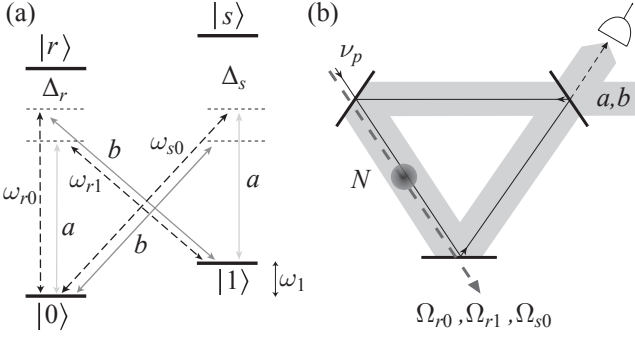


FIG. 1: (a) Atomic level and excitation scheme. (b) Potential ring-cavity setup. The laser fields (dashed lines) are at frequencies that are not supported by the resonator, but can be injected through one of the resonator mirrors so as to be co-propagating with the cavity fields through the ensemble.

The atom-light detunings  $\Delta_r = \omega_r - \omega_{r0}$  and  $\Delta_s = \omega_s - \omega_{s0}$  are taken to be much larger than any dipole coupling strengths, atomic linewidths, or cavity loss rates. This enables us to adiabatically eliminate the states  $|r\rangle$  and  $|s\rangle$  from the dynamics and neglect the effects of atomic spontaneous emission. Additionally, as depicted in Fig. 1, we assume that only three distinct Raman transitions are of significance (i.e., resonant or roughly resonant); i.e., we retain only those Raman processes that cause a change in the electronic state of the atoms ( $|0\rangle \rightarrow |1\rangle$  or  $|1\rangle \rightarrow |0\rangle$ ) and also involve transfer of a photon from a laser field to a cavity mode or vice-versa. All other possible Raman processes are assumed to be far off-resonant and therefore negligible. Finally, taking the wave numbers of the laser and cavity fields to be essentially equal, and introducing the collective spin operators  $J_z = \frac{1}{2} \sum_{j=1}^N (|1_j\rangle\langle 1_j| - |0_j\rangle\langle 0_j|)$ ,  $J_+ = \sum_{j=1}^N |1_j\rangle\langle 0_j|$ , and  $J_- = (J_+)^{\dagger}$ , we can derive a master equation for the cavity modes and ground-state atoms in the form

$$\dot{\rho}_g = -i[H_g, \rho_g] + \kappa_a D[a]\rho_g + \kappa_b D[b]\rho_g, \quad (2)$$

where  $D[A]\rho = 2A\rho A^\dagger - A^\dagger A\rho - \rho A^\dagger A$ ,  $\kappa_{a,b}$  are the cavity field decay rates, and (omitting constant energy terms)

$$H_g = \omega_0 J_z + \delta_a a^\dagger a + \delta_b b^\dagger b + 2\delta_a^- J_z a^\dagger a + 2\delta_b^- J_z b^\dagger b + \frac{\lambda_a}{\sqrt{N}} J_x (a + a^\dagger) + \frac{\lambda_b}{\sqrt{N}} (J_- b + J_+ b^\dagger), \quad (3)$$

with  $J_x = (J_+ + J_-)/2$  and

$$\omega_0 = \frac{|\Omega_{r1}|^2}{4\Delta_r} - \frac{|\Omega_{r0}|^2}{4\Delta_r} - \frac{|\Omega_{s0}|^2}{4\Delta_s} + \omega_1 - \omega'_1, \quad (4a)$$

$$\delta_a = \omega_a + \omega'_1 - \omega_{s0} + N\delta_a^+, \quad (4b)$$

$$\delta_b = \omega_b + \omega'_1 - \omega_{r0} + N\delta_b^+, \quad (4c)$$

$$\delta_a^\pm = \frac{|g_{s1}|^2}{2\Delta_s} \pm \frac{|g_{r0}|^2}{2\Delta_r}, \quad \delta_b^\pm = \frac{|g_{r1}|^2}{2\Delta_r} \pm \frac{|g_{s0}|^2}{2\Delta_s}, \quad (4d)$$

$$\lambda_a = \frac{\sqrt{N}\Omega_{r1}^* g_{r0}}{\Delta_r} = \frac{\sqrt{N}\Omega_{s0}^* g_{s1}}{\Delta_s}, \quad \lambda_b = \frac{\sqrt{N}\Omega_{r1}^* g_{r1}}{2\Delta_r}, \quad (4e)$$

where  $\omega'_1 = (\omega_{s0} - \omega_{r1})/2 \simeq \omega_1$ , and we have assumed the two Raman transitions involving mode  $a$  to occur at the same rate  $\lambda_a$ .

We now assume  $(\kappa_i^2 + \delta_i^2)^{1/2} \gg \lambda_a, \lambda_b, \omega_0$ . In this limit, the cavity modes are only weakly or virtually excited and may also be adiabatically eliminated to yield the following master equation for the reduced density operator,  $\rho$ , of the collective atomic system alone:

$$\dot{\rho} = -i[H_{LMG}^{\gamma=0}, \rho] + \frac{\Gamma_a}{N} D[2J_x]\rho + \frac{\Gamma_b}{N} D[J_+]\rho, \quad (5)$$

with  $h = -\omega_0/2$ ,  $\lambda = 2\lambda_a^2 \delta_a / (\kappa_a^2 + \delta_a^2)$ , and  $\Gamma_i = \lambda_i^2 \kappa_i / (\kappa_i^2 + \delta_i^2)$  ( $i = a, b$ ). Note that in deriving (5) we have also assumed that  $\kappa_b \gg \delta_b \simeq 0$ . If we then take  $\delta_a \gg \kappa_a$  and  $\Gamma_a \ll \Gamma_b$ , then the role played by each cavity mode in relation to the atomic system is quite distinct. Specifically, mode  $a$  mediates the collective spin-spin interaction (of strength  $\lambda \simeq \lambda_a^2/\delta_a$ ) associated with the Hamiltonian dynamics, whilst mode  $b$  mediates the collective atomic decay (with rate  $\Gamma_b \simeq \lambda_b^2/\kappa_b$ ).

The equations of motion for the moments  $\{\langle J_x \rangle, \langle J_y \rangle, \langle J_z \rangle\}$ , derived from (5), do not form a closed set. However, factorizing the means of operator products and taking the limit  $N \rightarrow \infty$  (i.e., neglecting quantum fluctuations), we obtain a closed set of semiclassical equations,

$$\dot{X} = 2hY - \Gamma_b ZX, \quad (6a)$$

$$\dot{Y} = -2hX + 2\lambda ZX - \Gamma_b ZY, \quad (6b)$$

$$\dot{Z} = -2\lambda XY + \Gamma_b (X^2 + Y^2), \quad (6c)$$

where  $(X, Y, Z) \equiv (\langle J_x \rangle, \langle J_y \rangle, \langle J_z \rangle)/j$  with  $j = N/2$ , and  $X^2 + Y^2 + Z^2 = 1$  (conservation of angular momentum). The stable steady-state solutions of (6) exhibit bifurcations at two critical effective field strengths,  $h_\pm^c = [\lambda \pm (\lambda^2 - \Gamma_b^2)^{1/2}]/2$  (we assume  $\lambda > 0, \Gamma_b$ ). In particular, for  $h < h_-^c$  and  $h > h_+^c$  the stable steady-state solutions are  $\{X_{ss} = Y_{ss} = 0, Z_{ss} = 1\}$ , whereas for  $h_-^c < h < h_+^c$  one finds

$$X_{ss} = \pm \sqrt{\frac{\Lambda^2 - 4h^2}{2\lambda\Lambda}}, \quad Y_{ss} = \frac{\Gamma_b}{\Lambda} X_{ss}, \quad Z_{ss} = \frac{2h}{\Lambda}, \quad (7)$$

where  $\Lambda = \lambda + (\lambda^2 - \Gamma_b^2)^{1/2}$ . Note that at both (supercritical pitchfork) bifurcations a detailed stability analysis

[15] shows that a unique steady state becomes unstable and two new stable steady states emerge. These semi-classical solutions, together with numerical solutions of the finite- $N$  master equation (5), are plotted in Fig. 2 as a function of  $h/\lambda$  (note that  $\langle J_x \rangle = \langle J_y \rangle = 0$  for the finite- $N$  calculations). The plots indicate both a first- and second-order phase transition *as a single parameter*,  $h$ , is varied. The first-order (second-order) transition, at  $h = h_-^c$  ( $h = h_+^c$ ), involves a discontinuous (continuous) bifurcation in  $X_{ss}$  and associated behavior in  $Z_{ss}$ . Note that in the purely Hamiltonian system second-order transitions occur at  $\pm h_+^c$ , but the first-order transition has no counterpart (for  $\lambda > 0$ ) and arises here due to a dissipative instability. The behavior we observe bears some relation to critical points found in cooperative resonance fluorescence (see, e.g., [13]).

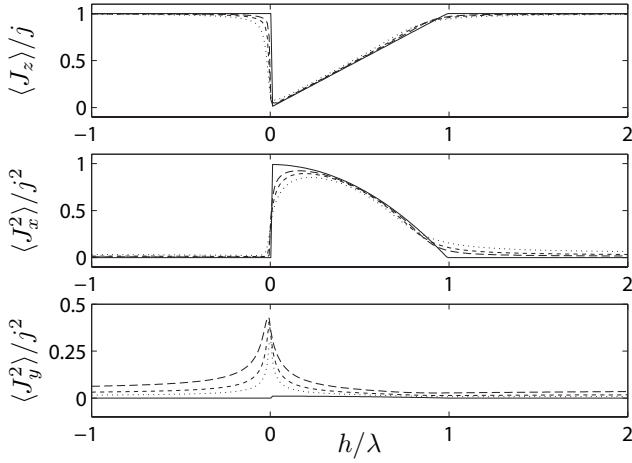


FIG. 2: Semiclassical (solid line) and finite- $N$  steady-state inversion and second-order moments for  $\Gamma_a/\lambda = 0.01$ ,  $\Gamma_b/\lambda = 0.2$ , and  $N = 25$  (dotted), 50 (short dash), 100 (long dash).

In the large- $N$  limit, quantum fluctuations can be included in the analysis as a first-order correction using a large- $N$  expansion of the Holstein-Primakoff (HP) representation of angular momentum operators [14]. Applied in a coordinate system where the mean Bloch vector points along the positive  $z$ -axis, this takes the form  $J_z = N/2 - c^\dagger c \simeq N/2$  and  $J_\pm = (N - c^\dagger c)^{1/2} c \simeq \sqrt{N} c$ , where  $c$  ( $c^\dagger$ ) is a bosonic annihilation (creation) operator. This linearization about the mean field state leads to a master equation of the general form

$$\begin{aligned} \dot{\rho} = & -i[H_{\text{HP}}, \rho] + \Gamma_+ D[c^\dagger] \rho + \Gamma_- D[c] \rho \\ & + \{ \Upsilon(2c\rho c^\dagger - c^2 \rho - \rho c^2) + \text{H.c.} \}, \end{aligned} \quad (8)$$

where  $H_{\text{HP}}$  is a quadratic in  $\{c, c^\dagger\}$  and the coefficients are functions of  $\{h, \lambda, \Gamma_a, \Gamma_b\}$  [15]. Eq. (8) yields coupled, linear equations of motion for  $\langle c \rangle$  and  $\langle c^\dagger \rangle$ , the eigenvalues of which display a sequence of bifurcations in both their real and imaginary parts as  $h$  is varied. The phase transitions are marked by the real part of one eigenvalue going to zero (i.e., critical slowing down) at  $h = h_\pm^c$ .

To examine this structure and dynamics, we consider the transmission of a (weak) probe laser field through the medium as a function of the probe frequency, i.e., we examine the frequency response of the system. A schematic of such a measurement setup is shown in Fig. 1(b). To compute the transmission spectrum we retain the two cavity modes in our model (i.e., we start from (2)), but again perform a linearization ( $N \gg 1$ ) about the mean-field state. We consider the case in which the probe laser drives mode  $b$ , and the transmission spectrum  $T_p(\nu_p)$  is defined as the coherent intensity, at probe frequency  $\nu_p$  (in the rotating frame), in the output field from mode  $b$ .

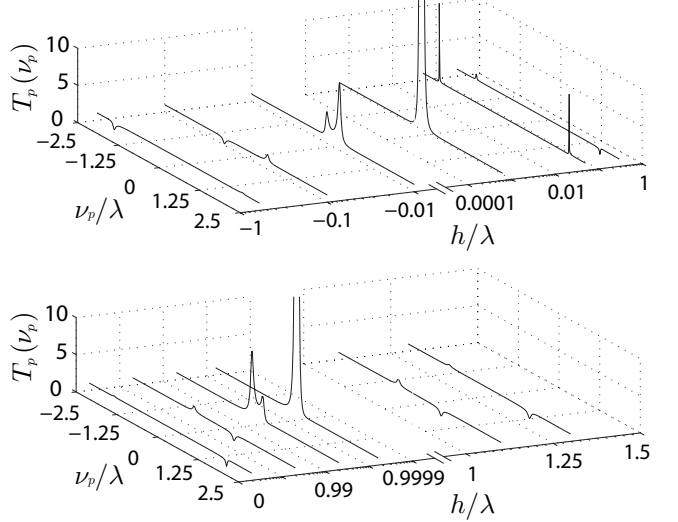


FIG. 3: Transmission spectra in the linearised regime, for  $h/\lambda = \{-0.6, -0.1, -0.01, h_-^c/\lambda, 0.05, 0.3\}$  (top), and  $\{0.5, 0.95, 0.995, h_+^c/\lambda, 1.1, 1.3\}$  (bottom), with microscopic parameters  $\kappa_a/\delta_a = 0.02$ ,  $\lambda_b/\lambda_a = 0.32$ ,  $\kappa_b/\delta_a = 1$ ,  $\delta_b = 0$ , giving  $\Gamma_a/\lambda = 0.01$ ,  $\Gamma_b/\lambda = 0.05$ . We set  $\delta_{a,b}^- = 0$ .

In Fig. 3 we plot  $T_p(\nu_p)$  (normalized by the maximum empty-cavity transmission) for a series of values of  $h$  around  $h_\pm^c$ . For the chosen parameters, the spectra consist of sharp “atomic” resonances superimposed on a much broader cavity mode resonance (i.e.,  $\kappa_b \gg \Gamma_b$ ). The locations and widths of the atomic resonances are determined by the imaginary and real parts of the above-mentioned eigenvalues, respectively. For  $|h/\lambda| > 1$ , the main atomic feature is a dip of width  $2\Gamma_b$  at  $\nu \simeq 2h$ , corresponding to a cavity-mediated, collective spontaneous emission resonance. For  $|h/\lambda| < 1$ , spin-spin interactions play a more significant role and a pair of resonances at opposite frequencies feature in the spectrum. As  $h \rightarrow h_+^c$  both from above and below these two features merge continuously into a single peak, centered at  $\nu_p = 0$ , which ultimately diverges at  $h = h_+^c$  in a pronounced signature of the second-order phase transition. The same merging and divergence is seen for the first-order transition, but only as  $h \rightarrow h_-^c$  from below. For  $h$  very small (but  $> h_-^c$ ), the spectrum consists of two sharp peaks of width

$\sim \Gamma_b h/\lambda$  at  $\nu_p \simeq \pm 2\lambda$ . The transition is signaled by a discontinuous jump from this two-peaked spectrum to a single divergent peak at  $\nu_p = 0$ .

To analyze the entanglement properties of the system, we adopt a criterion for bipartite entanglement in collective spin systems which, for symmetric states, is both necessary and sufficient, and reads [16]

$$C_\varphi \equiv 1 - (4/N)\langle \Delta J_\varphi^2 \rangle - (4/N^2)\langle J_\varphi \rangle^2 > 0, \quad (9)$$

where  $J_\varphi = \sin(\varphi)J_x + \cos(\varphi)J_y$ . Here, we present numerical results for  $C_R \equiv \max_\varphi C_\varphi (\geq 0)$ , which, in fact, equals the rescaled concurrence  $(N-1)C$ , where  $C$  is the two-spin concurrence. In Fig. 4 we plot the steady state value of  $C_R$  versus  $h/\lambda$ , computed from the linearized HP model and numerically from (5) for finite  $N$ . Both transitions are characterized by a sharp peak in the entanglement at the critical point [5, 6, 7], but they are distinguished by a discontinuity in  $C_R$  at  $h = h_-^c$  (for  $N \rightarrow \infty$ ) as opposed to a discontinuity in  $\partial C_R / \partial h$  at  $h = h_+^c$  [17]. The peaking of  $C_R$  at the critical points agrees with the conjecture of a general association between semiclassical bifurcations and maximal entanglement in dissipative, non-equilibrium many-body systems [18]. In the region where  $C_R = 0$  the state approaches a mixture of maximally polarised states possessing large fluctuations (see Fig. 2). Note that, in the adiabatic regime considered, the cavity field operator  $b(t) \propto J_+(t)$ , and so collective spin correlations (and hence  $C_R$ ) can be deduced from moments of the cavity output field, which may be measured by broadband homodyne detection.

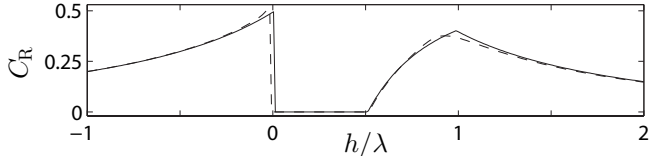


FIG. 4: Maximum entanglement  $C_R$  computed from the linearized HP ( $N \rightarrow \infty$ ) model (solid) and from (5) for  $N = 100$  (dashed), with  $\Gamma_a/\lambda = 0.01$  and  $\Gamma_b/\lambda = 0.2$ .

For an experimental realization, we have already mentioned  ${}^6\text{Li}$  in a ring-cavity setup. A suitable system can also be designed using the ground states  $|F = 1, m = \pm 1\rangle$  of  ${}^{87}\text{Rb}$  and linearly-polarized cavity modes [15]. For specific parameter values, we consider recent experiments with cold atoms inside a high-finesse optical ring cavity [19], i.e., we take  $g_{ij} \simeq 2\pi \cdot 100$  kHz and  $\kappa_a \simeq 2\pi \cdot 25$  kHz. For  $N \simeq 10^6$  atoms and a characteristic ratio  $\Omega_{ij}/\Delta_i \simeq 0.0025$ , we have  $\lambda_a \simeq 2\pi \cdot 250$  kHz. With a Raman detuning  $\delta_a \simeq 2\pi \cdot 2.5$  MHz, we then have  $\lambda \simeq 2\lambda_a^2/\delta_a \simeq 2\pi \cdot 25$  kHz and  $\Gamma_a \simeq \kappa_a(\lambda_a/\delta_a)^2 \simeq 2\pi \cdot 0.25$  kHz. Ground state magnetic level shifts of tens of MHz would suffice to ensure distinct Raman channels. Mode  $b$  may be more strongly damped (i.e., the two cavity polarizations have different finesse), e.g.,  $\kappa_b \simeq 2\pi \cdot 250$  kHz, and, with

$\lambda_b \simeq 2\pi \cdot 25$  kHz and  $\delta_b \simeq 0$ , we would then have  $\Gamma_b \simeq \lambda_b^2/\kappa_b \simeq 2\pi \cdot 2.5$  kHz  $\gg \Gamma_a$ . Finally, the rate for single-atom spontaneous emission (neglected in our model) is estimated by  $\Gamma_{\text{at}} \Omega_{ij}^2/(4\Delta_i^2) \lesssim 2\pi \cdot 0.01$  kHz  $\ll \lambda, \Gamma_b$  for an atomic excited state decay rate  $\Gamma_{\text{at}} = 2\pi \cdot 6$  MHz.

To conclude, we have proposed a feasible cavity QED system that is described by a dissipative LMG model and exhibits both first- and second-order non-equilibrium quantum phase transitions as a function of a single effective field parameter. Measurements on the cavity output light fields provide quantitative probes of the critical behavior. The system also offers opportunities for investigating phase transitions in response to variation of the strength of dissipation (i.e.,  $\Gamma_b$ ), for studying time-dependent behavior, such as entanglement dynamics, and for preparing very highly entangled states, which typically occur for short interaction times [15] and may in principle be “frozen” by switching off all optical fields.

The authors thank A. Daley and H. Carmichael for discussions and acknowledge support from the Austrian Science Foundation and from the Marsden Fund of the Royal Society of New Zealand.

---

- [1] I. Bloch, *Nature Phys.* **1**, 23 (2005).
- [2] A. Osterloh *et al.*, *Nature* **416**, 608 (2002).
- [3] T. J. Osborne and M. A. Nielsen, *Phys. Rev. A* **66**, 032110 (2002).
- [4] G. Vidal *et al.*, *Phys. Rev. Lett.* **90**, 227902 (2003).
- [5] J. Vidal, R. Mosseri, and J. Dukelsky, *Phys. Rev. A* **69**, 054101 (2004).
- [6] S. Dusuel and J. Vidal, *Phys. Rev. B* **71**, 224420 (2005).
- [7] J. Latorre *et al.*, *Phys. Rev. A* **71**, 064101 (2005).
- [8] R. G. Unanyan, C. Ionescu, and M. Fleischhauer, *Phys. Rev. A* **72**, 022326 (2005).
- [9] N. Lambert, C. Emary, and T. Brandes, *Phys. Rev. Lett.* **92**, 073602 (2004); *Phys. Rev. A* **71**, 053804 (2005).
- [10] J. Reslen, L. Quiroga, and N. F. Johnson, *Europhys. Lett.* **69**, 8 (2005).
- [11] H. J. Lipkin, N. Meshkov, and A. J. Glick, *Nucl. Phys.* **62**, 188 (1965).
- [12] F. Dimer *et al.*, *Phys. Rev. A* **75**, 013804 (2007).
- [13] R. Bonifacio and L. A. Lugiato, *Opt. Commun.* **19**, 172 (1976); P. D. Drummond and H. J. Carmichael, *Opt. Commun.* **27**, 160 (1978); H. J. Carmichael, *J. Phys. B* **13**, 3551 (1980).
- [14] T. Holstein and H. Primakoff, *Phys. Rev.* **58**, 1098 (1940).
- [15] S. Morrison and A. S. Parkins, arXiv:0711.2325
- [16] J. K. Korbicz, J. I. Cirac, and M. Lewenstein, *Phys. Rev. Lett.* **95**, 120502 (2005); *ibid.* **95**, 259901 (2005).
- [17] Note also that near  $h_+^c$  ( $h_-^c$ ) the entanglement  $C_\varphi$  is maximized around  $\varphi \simeq 0$  ( $\varphi \simeq \pi/2$ ).
- [18] S. Schneider and G. J. Milburn, *Phys. Rev. A* **65**, 042107 (2002).
- [19] Ch. von Cube *et al.*, *Fortschr. Phys.* **54**, 726 (2006); J. Klinner et. al, *Phys. Rev. Lett.* **96**, 023002 (2006)